Earthq Eng & Eng Vib (2008) 7:91-106 **DOI**: 10.1007/s11803-008-0785-z

Health monitoring of time-varying stochastic structures by latent components and fuzzy expert system

M. M. Ettefagh† and M. H. Sadeghi‡

Vibration and Modal Analysis Laboratory, Department of Mechanical Engineering, University of Tabriz, Tabriz 51666, Iran

Abstract: In this paper, a novel parametric model-based decomposition method is proposed for structural health monitoring of time-varying structures. For this purpose, the advanced Functional-Series Time-dependent Auto Regressive Moving Average (FS-TARMA) technique is used to estimate the parameters and innovation variance used in the parametric signal decomposition scheme. Additionally, a unique feature extraction and reduction method based on the decomposed signals, known as Latent Components (LCs), is proposed. To evaluate the efficiency of the proposed method, numerical simulation and an experimental study in the laboratory were conducted on a time-varying structure, where various types of damage were introduced. The Fuzzy Expert System (FES) was used as a classification tool to demonstrate that the proposed method successfully identifies different structural conditions when compared with other methods based on non-reduced and ordinary feature extraction.

Keywords: parametric modeling; signal decomposition; feature extraction/reduction; fuzzy classification

1 Introduction

From a physical standpoint, the time-dependent/or inherently nonlinear dynamics of stochastically-excited systems causes Nonstationary Stochastic Vibration (NSV). These systems are frequently encountered in practice, and include earthquake-excited vibration, vibration of surface vehicles, airborne structures, sea vessels, rotating machinery, and so on. From a mathematical point of view, NSV is characterized by time-dependent statistical moments. Modeling and analysis of these systems, based on available signal measurements and by considering the non-stationary effect, is very important in a wide variety of applications including Structural Health Monitoring (SHM). Recently, SHM has received significant attention from the research community. Depending upon the physical system itself, the model (parametric or non-parametric) used, and the decision-making mechanism, vibration-based SHM methods may be classified in various ways (Sakellariou and Fassois, 2006).

Non-parametric methods are based upon non-parameterized representation of the vibration energy as a simultaneous function of time and frequency (time-frequency distribution). These methods include the classical short Fourier transform to wavelet-based method introduced by Qian and Chen (1996). Parametric methods are, on the other hand, based upon parameterized representations of the Time-dependent Autoregressive Moving Average (TARMA) or related types, and offer a number of advantages (Poulimenos and Fassois, 2006) such as: improved accuracy; improved resolution; improved tracking of the time-varying dynamics; and flexibility in analysis, as they are capable of directly capturing the underlying structural dynamics responsible for the nonstationary behavior.

Recently, some non-parametric methods have been proposed, based on nonstationary signal decomposition, to extract meaningful information from vibration signals. Two major decomposition methods have been reported in the literature. One method, proposed by Strang and Nguyen (1996), is based on the Discrete Wavelet Transform (DWT), and permits systematic decomposition of a signal into its sub-band levels. Suitable feature extraction is then achieved using the method introduced by Serhat and Fmine (2003). However, wavelet analysis is essentially an adjustable windowed Fourier transform and due to length limitations of the wavelet bases, energy leakage could occur in wavelet transformation (Vincent *et al.*, 1999). Furthermore, once the wavelet bases and the decomposition scales are determined, the wavelet transform results in a signal with a certain scale, whose frequency components are related to the sampling

Correspondence to: Mir Mohammed Ettefagh, Vibration and Modal Analysis Laboratory, 51666-14766, Department of Mechanical Engineering, University of Tabriz, Tabriz, Iran
Tel: 989144064291; Fax: +984113356026
E-mail: ettefagh@tabrizu.ac.ir
†PhD Candidate; ‡Assistant Proffesor

Received November 11, 2007; **Accepted** December 29, 2007

frequency but not to the signal itself. Therefore, wavelet analysis is not a self-adaptive signal processing method. Another method, recently proposed by Huang (1998), is Empirical Mode Decomposition (EMD), which decomposes a signal into a set of complete and almost orthogonal components called Intrinsic Mode Functions (IMF) that are almost mono-component. By using the Hilbert Transform (HT) on the IMFs, an elaborate energy-frequency-time distribution of the signal, i.e., Hilbert-Huang Transform (HHT) spectrum, is obtained. Also, an accurate feature extraction method can be applied to the IMFs or HHT for monitoring (Yu *et al.*, 2006). EMD is a self-adaptive signal processing method that can be applied to both nonlinear and nonstationary processes, which has overcome the limitations of the Fourier transform and has a high SNR.

The features, extracted using the decomposition methods (DWT and HHT) mentioned above, are based on non-parametric models. On the other hand, parametric nonstationary modeling and analysis methods can achieve high performance characteristics and benefits that cannot be obtained using their non-parametric counterparts. This statement is proven elsewhere (Poulimenos and Fassois, 2006; Zhan and Jardine, 2005), where the NSV signal is shown to be from structural and rotating time-varying systems, respectively. Thus a decomposition method based on parametric modeling that decomposes the structural NSV signal into a collection of components would be very useful for accurate feature extraction or dimension reduction, and consequently for use in SHM. A method, based on the Time-dependent Auto Regressive (TAR) model, has been proposed by West and Harrison (1997) to decompose the nonstationary time-series into components. The resulting components are called Latent Components (LCs). Prado (1998) utilized a "stochastic parameter evaluation structure" in this method to estimate the TAR model parameters. The application of the LCs in feature extraction for EEG signal analysis is reported in West *et al.* (1999) and condition monitoring of the sheet metal stamping process is described in Li and Du. (2005).

Although decomposition of the nonstationary time-series based on a parametric model has been addressed, there was no attempt to use LCs to analyze the structural NSV signal. Also, applying the TARMA parametric modeling and using a Deterministic Parameter Evaluation (DPE) structure have not been considered for estimating model parameters in LC applications. Therefore, using LCs as a feature extraction and dimension reduction tool based on TARMA modeling is highly desirable for use in SHM methods. Note that an information-based method was previously proposed by Sadeghi and Fassois (1997, 1998) and Rahimi *et al.* (2007) to reduce the dimension of the features, extracted by a parametric-based method and applied in SHM of stationary structures. However, there are no parametric-based SHM methods that can be applied to a time-varying stochastic structural system.

In this paper, by using a DPE structure of the TARMA model that was proven to be accurate and appropriate for vibration analysis, and applying a two-Stage Least Square with Prediction Error (2SLS-PE) estimation method (Poulimenos and Fassois., 2006), the parametric-based decomposition method described above is applied to an NSV signal to produce LCs. Then, the extracted LCs are used as the inputs to the Fuzzy Expert System (FES) (Pawar and Ganguli, 2007) to classify the condition of the system. This method is successfully applied to a stochastic time-varying 3-DOF system. In addition, to justify the proposed method in practical situations, an experimental setup using a stochastic time-varying structure was carried out. Different classes of damage were assumed to be created by different conditions of the structure's mass or stiffness shifting from their nominal values. Thus, the research described herein (i) introduces a proper and effective method that is based on LCs of a stochastic time-varying system's signal for feature extraction/or reduction using advanced TARMA parametric modeling; (ii) shows the effective handling of uncertainties via parametric modeling and the FES; and (iii) presents a simplified health monitoring system for time-varying stochastic structures based on fuzzy classification.

The remainder of this paper is organized as follows. Nonstationary signal decomposition theory using a TARMA model with a DPE structure and the 2SLS estimation method is described in Section 2. To verify the proposed method, a numerical simulation and laboratory testing of a time-varying 3DOF structure are carried out and described in Sections 3 and 4, respectively. Conclusions are given in Section 5.

2 LC theory

2.1 Nonstationary signal decomposition theory using parametric model

It is assumed that a Nonstationary signal $x[t]$ follows a TAR model on the order of p:

$$x[t]=\sum_{j=1}^{p}\phi_{t,j}x[t-j]+\varepsilon[t] \qquad (t=1,2,...) \tag{1}$$

where $\boldsymbol{\varphi}_t=\left[\phi_{t,1}\ \phi_{t,2}\ ...\ \phi_{t,p}\right]^{\mathrm{T}}$ is the TAR parameters vector at time t and $\varepsilon[t]$ is a zero-mean innovation. The innovations are assumed to be uncorrelated and normal, $\varepsilon[t]\sim N(0,\sigma_t^2)$, with time-dependent variances σ_t^2. The model has the form of a standard Auto Regressive (AR) at each time instant, but the AR parameters and innovations variance may change throughout the process. The model is very general, permitting both slow and more rapid or abrupt changes in parameters, and as a result, provides a very flexible framework for modeling patterns of change in the stochastic structure

and observed non-stationary behavior in the signal. The model is completed by specifying evolution model structures for the time-dependent parameters $\boldsymbol{\varphi}_t$ and the innovations variance σ_t^2; this is discussed in detail in Section 2.2. The theoretical basis of the decomposition methodology and its implications in the class of TAR models, denoted by Eq. (1) irrespective of the specific forms of evolution of $\boldsymbol{\varphi}_t$ and σ_t^2, are described next.

The theory is accessed by casting the TAR model (see Eq. (1)) in Dynamic Linear Model (DLM) form (West and Harrison, 1997) as follows:

$$x[t]=\boldsymbol{F}^{\mathrm{T}}\boldsymbol{x}_t,\quad \boldsymbol{x}_t=\boldsymbol{G}_t\boldsymbol{x}_{t-1}+\boldsymbol{\omega}_t \tag{2}$$

where $\boldsymbol{F}=[1\ 0\ ...\ 0]^{\mathrm{T}}$, $\boldsymbol{x}_t=[x[t]\ x[t-1]\ ...\ x[t-p+1]]^{\mathrm{T}}$, $\boldsymbol{\omega}_t=\varepsilon[t]\boldsymbol{F}$, and

$$\boldsymbol{G}_t\equiv \mathrm{G}(\boldsymbol{\phi}_t)=\begin{bmatrix}\phi_{t,1} & \phi_{t,2} & \phi_{t,3} & \cdots & \phi_{t,p-1} & \phi_{t,p}\\ 1 & 0 & 0 & ... & 0 & 0\\ 0 & 1 & 0 & ... & 0 & 0\\ . & & & . & & .\\ . & & & . & 0 & .\\ . & & & . & & .\\ 0 & 0 & ... & ... & 1 & 0\end{bmatrix}$$

This is one of the several possible DLM forms of the TAR model and a natural extension of the DLM representation of standard AR models. The central decomposition is achieved from the standard theory of model structures and similar models in linear stochastic systems (West and Harrison, 1997). It is supposed that at each time instant t, the eigenvalues of $\boldsymbol{G}_t$ are distinct, as is generally true for TAR models of practical interest. The distinct eigenvalues usually contain complex elements. Also, there are c pairs of complex conjugate eigenvalues and $r=p-2c$ real and distinct eigenvalues. The numbers of real and complex eigenvalues may differ at different t, but it is assumed herein that they are fixed in number, so c and r are not subscripted by t. The complex eigenvalues are denoted by $r_{t,j}\exp(\pm \mathrm{i}\omega_{t,j})$ for j=1,...,c, and the real eigenvalues by $r_{t,j}$ for j=2c+1,...,p. Then $\boldsymbol{G}_t=\boldsymbol{E}_t\boldsymbol{A}_t\boldsymbol{E}_t^{-1}$, where $\boldsymbol{A}_t$ is the diagonal matrix of eigenvalues, in the arbitrary order specified, and $\boldsymbol{E}_t$ is the $p\times p$ matrix whose columns are the corresponding normalized eigenvectors. The model Eq. (2) is re-parameterized by defining the matrix $\boldsymbol{H}_t$ as follows:

$$\boldsymbol{H}_t=\mathrm{diag}(\boldsymbol{E}_t\boldsymbol{F})\boldsymbol{E}_t^{-1} \tag{3}$$

and $\boldsymbol{x}_t$ is linearly transformed to $\boldsymbol{\gamma}_t$ through $\boldsymbol{H}_t$ as follows:

$$\boldsymbol{\gamma}_t=\boldsymbol{H}_t\boldsymbol{x}_t \tag{4}$$

Then Eq. (2) becomes:

$$x[t]=\boldsymbol{I}^{\mathrm{T}}\boldsymbol{\gamma}_t,\quad \boldsymbol{\gamma}_t=\boldsymbol{A}_t\boldsymbol{K}_t\boldsymbol{\gamma}_{t-1}+\boldsymbol{\delta}_t \tag{5}$$

where $\boldsymbol{I}=[1\ 1\ ...\ 1]^{\mathrm{T}}$, $\boldsymbol{\delta}_t=\boldsymbol{H}_t\boldsymbol{\omega}_t$, $\boldsymbol{\gamma}_t=[\gamma_{t,1}\cdots\gamma_{t,p}]^{\mathrm{T}}$ and $\boldsymbol{K}_t=\boldsymbol{H}_t\boldsymbol{H}_{t-1}^{-1}$. This means that $x[t]$ is the sum of the individual $\gamma_{t,j}$ processes. By construction, the final r elements of $\boldsymbol{\gamma}_t$ are real, corresponding to the real eigenvalues $r_{t,j}$ at each time t. Also, these real processes are renamed as $y_{t,j}$. In addition, the initial 2c elements of $\boldsymbol{\gamma}_t$ occur as complex conjugate pairs. Within each pair j=1,...,c, the sum $z_{t,j}=\gamma_{t,2j-1}+\gamma_{t,2j}$ is real and is simply evaluated as twice the common real part. Each real process $z_{t,j}$ corresponds to the eigenvalue pairs at time $r_{t,j}\exp(\pm \mathrm{i}\omega_{t,j})$. Finally, the basic decomposition result may now be expressed as (Prado, 1998):

,

$$x[t]=\sum_{j=1}^{c}z_{t,j}+\sum_{j=1}^{r}y_{t,j} \tag{6}$$

where the values of each of the real processes $z_{t,j}$ and $y_{t,j}$ may be evaluated directly based on the foregoing theory. For known, estimated or simulated values of $\boldsymbol{F}$, $\boldsymbol{G}_t$ and $\boldsymbol{x}_t$ at each time t, the processes $z_{t,j}$ and $y_{t,j}$ can be evaluated over time by computing the eigenstructure of the evolution matrix $\boldsymbol{G}_t$ and the transformations described above (Eq. (4)). Exploring the structure of these processes over time provides insight in understanding the structure of the underlying signal $x[t]$. In the general case of TAR, each $y_{t,j}$ process follows a TAR(1) (Prado, 1998):

$$y_{t,j}=r_{t,j}y_{t-1,j}+\delta_{t,2c+j}\qquad j=1,...,r \tag{7}$$

with TAR parameter, $r_{t,j}$, at time t. Similarly, $z_{t,j}$ follows a TARMA(2,1):

$$z_{t,j}=2r_{t,j}\cos(\omega_{t,j})z_{t-1,j}-r_{t,j}^2z_{t-2,j}+\eta_{t,j}\qquad j=1,...,c \tag{8}$$

whose amplitude and phase changes randomly over time. Also, the frequencies $\omega_{t,j}$ and the module $r_{t,j}$ for each j are time-dependent and are known as Instant Frequency (IF) and Instant Module (IM), respectively. Note that the innovations of the abovementioned processes ($\delta_{t,j}$ and $\eta_{t,j}$) in Eqs. (7) and (8) are all multiples of the original innovation $\varepsilon[t]$ The series $x[t]$ is then decomposed as a sum of TAR(1) and quasi-cyclical TARMA(2,1), which are known as LCs.

2.2 TARMA model with DPE structure and 2SLS estimation method

Identification of the TAR model in Eq. (1), as a parametric model, requires structuring of the time evolutions of $\boldsymbol{\varphi}_t$ and σ_t^2 among other things. Generally, parametric models may be further classified according

to the type of structure imposed upon the evolution of the time-dependent model parameters ($\boldsymbol{\varphi}_t$ and σ_t^2). In this study, the Functional-series Time-dependent Auto Regressive Moving Average (FS-TARMA), in DPE form, were applied to construct the $\boldsymbol{\varphi}_t$ and σ_t^2 for the first time; whereas in previous research concerning LC theory and its applications, stochastic parameter evolution structures have been applied without using the TARMA model to estimate $\boldsymbol{\varphi}_t$ and σ_t^2.

It should also be mentioned that in this paper, the TAR parameters are estimated indirectly through the TARMA parameter estimation algorithm and result in an optimum TAR model structure. This optimality stems from the fact that the time-varying mechanical systems can be optimally modeled by TARMA models. Thus, directly modeling TAR without using TARMA models will result in an unnecessarily high order and suboptimum model (Poulimenos *et al*., 2006). In the following, the FS-TARMA model with the DPE structure and 2SLS estimation method is summarized.

The DPE structure is achieved by postulating the parameters of the TARMA model as deterministic functions of time, belonging to a specific Functional Subspace (FS). Their AR, Moving Average (MA) parameters, as well as their innovations variance, are all expanded within a properly selected FS defined as (Poulimenos *et al*., 2006):

$$F_{AR} \triangleq \left\{G_{b_a(1)}[t], G_{b_a(2)}[t], ..., G_{b_a(p_a)}[t]\right\},$$

$$F_{MA} \triangleq \left\{G_{b_c(1)}[t], G_{b_c(2)}[t], ..., G_{b_c(p_c)}[t]\right\},$$

$$F_{\sigma_e^2} \triangleq \left\{G_{b_s(1)}[t], G_{b_s(2)}[t], ..., G_{b_s(p_s)}[t]\right\}.$$

In these expressions "F" designates FS of the indicating quantity and $G_j[t]$ is a set of orthogonal basis functions selected from a suitable family (such as Chebyshev, Legendre, trigonometric). The AR, MA and variance subspace dimensionalities are indicated as p_a, p_c and p_s respectively, while the indices $b_a(i)(i=1,..,p_a)$, $b_c(i)(i=1,..,p_c)$ and $b_s(i)(i=1,..,p_s)$ designate the specific basis functions of a particular family that are included in each subspace. The time-dependent AR, MA and innovations variance of an FS-TARMA $(n_a, n_c)_{[p_a,p_c,p_s]}$ representation may be thus expressed as:

$$\begin{cases} a_i[t] = \sum_{j=1}^{p_a} a_{i,j} G_{b_a(j)}[t] \\ c_i[t] = \sum_{j=1}^{p_c} c_{i,j} G_{b_c(j)}[t] \\ \sigma_e^2[t] = \sum_{j=1}^{p_s} s_j G_{b_s(j)}[t] \end{cases} \tag{9}$$

with $a_{i,j}$, $c_{i,j}$ and s_j designating the AR, MA and innovations variance, respectively, coefficients of projection.

The problem of parameter estimation in FS-TARMA models consists of determining the AR/MA and innovations variance projection coefficient vectors $\boldsymbol{v}$ and $\boldsymbol{s}$, respectively, which was formulized and described by Poulimenos and Fassois (2003, 2005 and 2006). Note that an Akaike Information Criterion-based scheme, known as integer optimization (Akaike, 1977), is applied for optimum structure selection of the FS-TARMA models. In addition, once the model is obtained, it must be validated. Although this may be based on various methods, formal validation procedures are typically based upon the posterior examination of the underlying assumptions, such as a model's residual (PE) uncorrelatedness (whiteness) and Gaussianity test. But, due to the residual time-dependent variance, the usual residual whiteness tests may not be applicable in the nonstationary case. Therefore, another test may be applied, based upon the number of sign changes in the series $e[t, \hat{\upsilon}]$ (Draper and Smith, 1998).

After estimating these parameters, the desired optimum estimation of $\boldsymbol{\varphi}_t$ and σ_t^2 can be found based on the inverse function coefficients of projection, associated with the FS-TARMA model (Poulimenos and Fassois, 2006). Therefore, using this proposed procedure, the FS-TARMA model with DPE structure and 2SLS estimation method, known as the best method for modeling the nonstationary stochastic vibration signal, is directly used to decompose the signal. In other words, by using the proposed algorithm, accurate parameters and innovation variance may be found, so it is possible to achieve the optimum TARMA and consequently the optimum TAR model with minimum order. Clearly, LCs of the signal, extracted due to signal decomposition, can give more accurate and informative features for further evaluation of the nonstationary stochastic vibration signal.

3 Applying the proposed method to a stochastic time-varying 3-DOF system

In this section, the proposed method is applied to a simulated time-varying 3-DOF system to verify its ability to identify the condition of the system.

3.1 Simulation and FS-TARMA mosdeling of the NSV signal

A time-varying 3-DOF viscously damped system, which was also used by Poulimenos and Fassois (2006), is considered as a benchmark in this work. Fig.1 schematically shows this system, which is subjected to an unobservable displacement excitation $r(t)$. The system is time-varying, as the stiffness $k_2(t)$ and $k_3(t)$ change with time in the following manner:

$$k_i(t) = k_{i,0} + k_{i,1}.\sin(2\pi t / P_{i,1}) + k_{i,2}.\sin(2\pi t / P_{i,2}) \quad (i = 2,3) \tag{10}$$

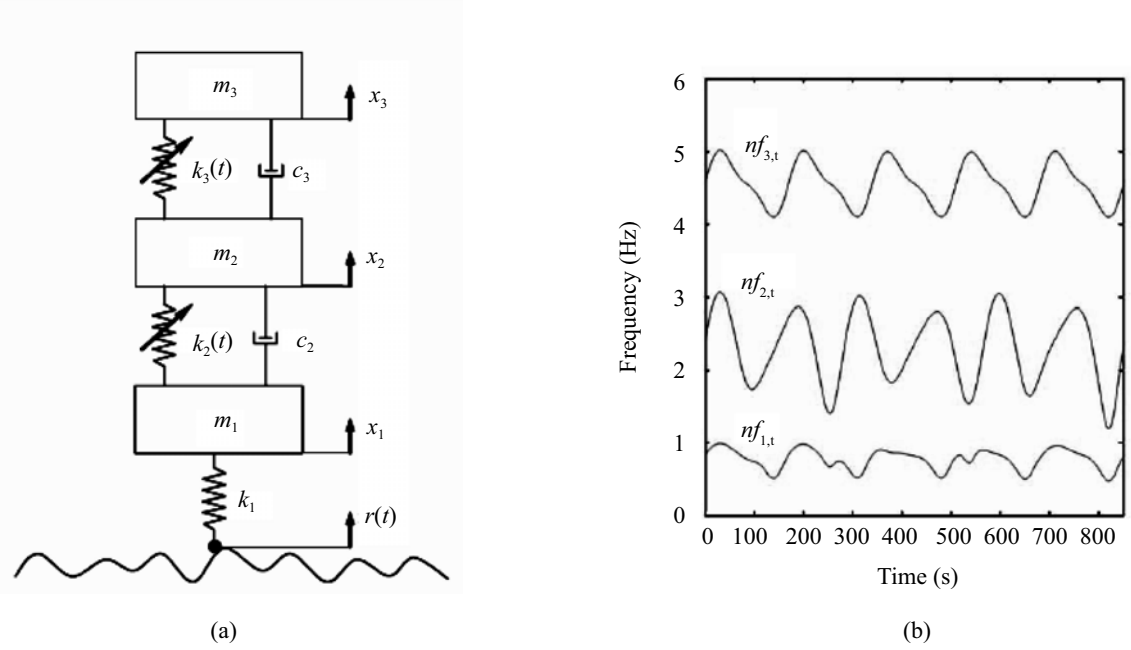

Fig. 1 Schematic diagram of time-varying mechanical system (a) and natural frequencies of the system (b)

with $P_{i,1}$ and $P_{i,2}$ designating the periods in the time-variation. The numerical values of $k_{i,0}$, $k_{i,1}$, $k_{i,2}$ $P_{i,1}$, $P_{i,2}$ and also the details of the simulation process can be found in Poulimenos *et al*. (2006). Given a particular excitation realization, the system equations are integrated (for $t \in [16.67, 850]$ s) via the Runge–Kutta 4/5 method characterized by variable integration steps, and are subsequently recorded with 48 samples per second (Poulimenos and Fassois, 2006). Also, the obtained displacement response, $x_3(t)$, is low-pass filtered via a Chebyshev II filter with a cut-off frequency of 6 Hz, and re-sampled at f_s=12Hz. In order to minimize the initialization effects, the initial 200 samples (16.67 s) of the response signal are discarded. Each nonstationary response realization is thus $\Delta t = 850$ s.

The optimal AR and MA model orders are selected as n_a=6 and n_c=3, respectively. Also, the AR, MA and innovations variance functional subspaces are of dimensionalities p_a=41, p_c=2 and p_s=19, respectively, in the forms mentioned in Poulimenos and Fassois. (2006).

3.2 Structure damage simulation, feature extraction and reduction

It is well known that a flaw in a structural system changes its mass or stiffness, so a method that can identify variations in the mass or stiffness of a system in considered reliable for health monitoring purposes. However, a note of precaution is important. The scheme should be able to discriminate between the time-varying nature of the system parameters, and the damage that may happen in the course of operation that changes the parameters. As the results will show, the pattern of these two types of changes is different and distinguishable. Here, different damage classes of the structure are simulated by decreasing the mass or stiffness of the system. In this simulation, normal mode operation plus 18 classes of damage are defined. The damage is defined according to its type, location and severity as listed in Table 1. After simulation of 19 operational classes, the parameters $\boldsymbol{\varphi}_t$'s and the variances σ_t^2's for each class are estimated. Then, by constructing $\boldsymbol{\varphi}_t$ and σ_t^2, the LCs of the NSV signals are extracted.

In previous studies (Prado, 1998 and West *et al.*, 1999), two major sets of features associated with LCs of the NSV signals have been considered. One set is related to the IF, $\omega_{t,j}$, and the other corresponds to the IM, $r_{t,j}$, of each LCs (see Eqs. (7) and (8)). In this work, a combination of the IF and IM, $2r_{t,j}\cos(\omega_{t,j})$, is used as a new set of features. It is expected that this new form of feature set is more informative than previous ones, because the time-evolution behavior of the combined $\omega_{t,j}$ and $r_{t,j}$ is more informative than $\omega_{t,j}$ and $r_{t,j}$ alone. This idea is confirmed by comparing the Success Rate (SR) of the classification when different sets of features are selected. In the following, Feature Set 1 (FS1), S_{F1} Feature Set 2 (FS2), S_{F2}, and Feature Set 3 (FS3), S_{F3} are denoted as the Feature Sets corresponding to the $\omega_{t,j}$, $r_{t,j}$ and AR(2) part of NSV signal's LCs, respectively.

After implementing the proposed decomposition method on the NSV signal in each scenario of the structure damage class, it is recognized that the number of distinct eigenvalues, mentioned in Section 2.1, is p=2c+r=20, in which 2×(c=9) eigenvalues are complex and the remaining eigenvalues r=2 are real. As shown, in deriving the theory basis of the LCs, it is essential to assume that the number of real and complex eigenvalues is constant during the time evolution. Although the number of the real or complex pairs of eigenvalues may differ at different times in real situations, this issue can

Table 1 Linguistic classification of structure conditions in the simulated time-varying 3-DOF system.

Class number	Rule	Decreasing rang
1	Normal	–
2	Small decrease in m_1	10-25 present reduction
3	Considerable decrease in m_1	25-50 present reduction
4	Very high decrease in m_1	50-70 present reduction
5	Small decrease in m_2	10-25 present reduction
6	Considerable decrease in m_2	25-50 present reduction
7	Very high decrease in m_2	50-70 present reduction
8	Small decrease in m_3	10-25 present reduction
9	Considerable decrease in m_3	25-50 present reduction
10	Very high decrease in m_3	50-70 present reduction
11	Small decrease in k_1	10-25 present reduction
12	Considerable decrease in k_1	25-50 present reduction
13	Very high decrease in k_1	50-70 present reduction
14	Small decrease in k_2	10-25 present reduction
15	Considerable decrease in k_2	25-50 present reduction
16	Very high decrease in k_2	50-70 present reduction
17	Small decrease in k_3	10-25 present reduction
18	Considerable decrease in k_3	25-50 present reduction
19	Very high decrease in k_3	50-70 present reduction

be circumvented by considering the switching effect (see Prado, 1998 and West *et al.*, 1999), which is discussed in detail after the LCs of the signal have been obtained.

Figure 2 shows the S_{F1}, S_{F2} and S_{F3}, i.e. FS1, FS2 and FS3 of the obtained LCs of the NSV signal in the undamaged condition of the system. The extracted LCs of the NSV signal ($z_{t,j}$) can be sorted in increasing or decreasing order of the IF value. Here, the LCs of the system are sorted with IF decreasing order (Fig. 2(a)). Also, the trajectories of nine LCs with the corresponding numbers (on every trajectory) are shown. Note that there is a relationship between the IF and the natural frequency of the 3-DOF system, but the exact correspondence is not a concern in this paper. It only occurs if the natural frequency is assumed to be $nf_{j,t} = \alpha_{j,t}\cos(\beta_{j,t}\ t) + A_j$ ($\alpha_{j,t}$, $\beta_{j,t}$, and $A_{j,t}$ are the time-varying parameters, corresponding to the jth natural frequency). Then, the IF will be $\omega_{j,t} = K_j\alpha_{j,t}\cos(\beta_{j,t}\ t) + K_j'A_j$, where K_j and K_j' are constants, which are not known precisely. This idea is confirmed by comparing the IF in Fig. 2(a) with the natural frequencies of the system shown in Fig. 1(b).

Two complications arise in moving from the TAR parameters to the feature sets (Prado, 1998; West *et al.*, 1999). The first complication is that there is no inherent mathematical identification of the roots, and so no immediate identification of the corresponding LCs. As frequency and amplitude characteristics of the LCs vary through time, a component that has the lowest frequency at one time instant may later have a higher frequency, for example. Similar concerns apply to the module and the amplitudes of the components. This effect is known as "switching" over the course of a time series. The second complication is that the number of real/complex pairs of eigenvalues may differ at different times. The analysis described in Section 2 assumed fixed and constant numbers of r and c, so the decomposition follows easily, but complications can arise as these numbers change. The key reason is that collections of higher frequency components $z_{t,j}$ corresponding to complex roots will often have a fairly low module $r_{t,j}$ and are apparent in the model decomposition as representations of high frequency noise; these are important model components but are typically low in amplitude relative to the more dominant, lower-frequency, and persistent components that have physical interpretations. With very high-frequency ranges, relatively small changes in TAR parameters can lead to one or more pairs of such complex roots disappearing, replaced by real roots with low values and correspondingly low amplitudes of the induced real components in the series. The reverse of this phenomenon, complex roots substituting real roots,

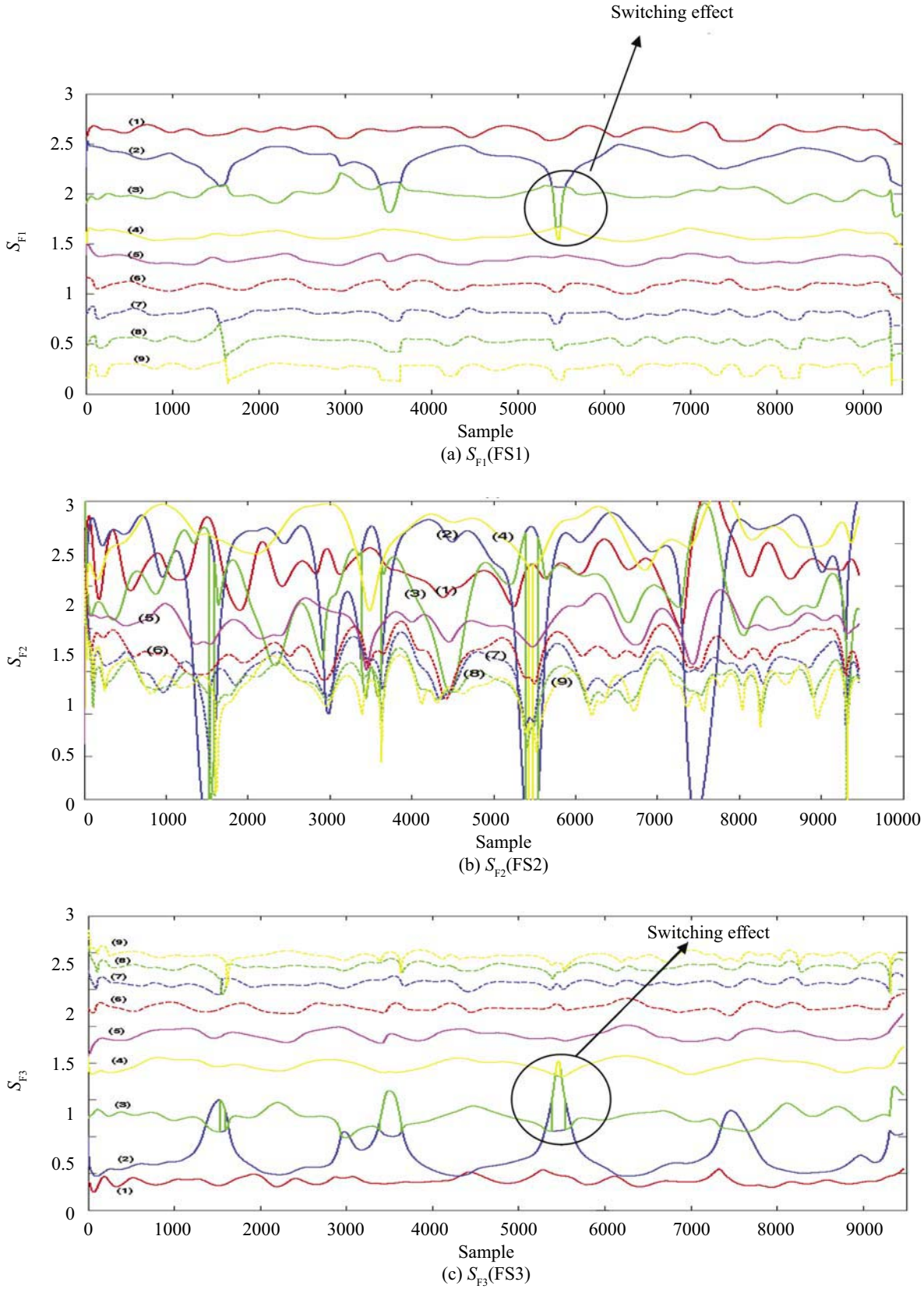

Fig. 2 Trajectories of extracted feature sets, associated with the obtained LCs (The number of LCs is inside the parenthesis), in decreasing order of IF for different undamaged cases

also occurs. This methodological phenomenon must be recognized, although its practical importance may be negligible. By observing Fig. 2, the first complication (the switching effect) is evident, especially in the

feature sets, corresponding to the second and third LCs. For example, as shown by a circle in Fig. 2, when the frequency drops in a given region, the second LC is switched to the third LC. The second complication (varying the number of the eigenvalues/ or characteristic roots) is not observed in this work (except for a short time, which is not significant) when the NSV signal is decomposed.

In addition, note that in general, an informative LC has a high module, whereas a low-module LC corresponds to the inherent or non-inherent noise of the system (here non-inherent noise is referred to as those components of the signal which originate from the unmodeled part of the signal.). For example, as seen in Fig. 2(b), LCs #5, #6, #7, #8 and #9, which correspond to the lower IF, have generally low modules in comparison with the first four LCs (#1, #2, #3 and #4). Hence, to reduce the features dimension, the first four LCs can be considered as the informative features and are retained whereas the other LCs may be eliminated. Therefore an "informal" method to reduce the number of extracted LCs is to eliminate those LCs with very low modules. This feature reduction method is one of the important achievements of this research and as shown later, the proposed method considerably increases the SR of the classification.

Figure 3 show trajectories of extracted S_{F3}(FS3), associated with the obtained LCs in different scenarios of structure conditions. The individual pattern of each class of structure condition can be distinguished from a general view of the retained features in these figures. For example, the major distinguishing pattern of the third class is seen first when the LC gets close to the second one; oscillatory behavior with low frequency and high amplitude of the fourth LC is the unique pattern of the 6th and 9th classes, while mixing the third LC with the fourth LC is more apparent in the 9th class; increasing the distance of the first LC from the second LC is the distinctive pattern of the 12th and 15th classes, while mixing the second LC with the third LC is more apparent in the 15th class; and being smooth without any major oscillatory behavior (with low frequency) is the main pattern of the 18th class. In addition, it is very difficult to find distinguishable patterns for each class by just considering the delimited features. Also, by producing a similar figure (for brevity, these figures are not included in this paper) for other feature sets (FS1 and FS2), the individual pattern is not very clear.

By defining the numerical values of these feature sets, the FES may be used to identify the class of the structure condition. The numerical values, denoted as Numerical Values (NV), V_{NV} are:

NV of all feature sets

NV of retained feature sets

$$V_{NV1}=\left|\text{Mean}(1^{st}\ \text{LC})-\text{Mean}(2^{nd}\ \text{LC})\right|\ \text{("Mean" imply the mean value of the LC);}$$
$$V_{NV2}=\left|\text{Mean}(2^{nd}\ \text{LC})-\text{Mean}(3^{rd}\ \text{LC})\right|;$$
$$V_{NV3}=\left|\text{Mean}(3^{rd}\ \text{LC})-\text{Mean}(4^{th}\ \text{LC})\right|;$$
$$V_{NV4}=\left|\text{Var}(1^{st}\ \text{LC})\right|;\ \text{("Var" imply the variance value of the LC);}$$
$$V_{NV5}=\left|\text{Var}(2^{nd}\ \text{LC})\right|;$$
$$V_{NV6}=\left|\text{Var}(3^{rd}\ \text{LC})\right|;$$
$$V_{NV7}=\left|\text{Var}(4^{th}\ \text{LC})\right|;$$
$$V_{NV8}=\left|\text{Mean}(4^{th}\ \text{LC})-\text{Mean}(5^{th}\ \text{LC})\right|$$
$$V_{NV9}=\begin{cases}0 & \text{if } \left|\text{Mean}(1^{st}\ \text{LC})-\text{Mean}(2^{nd}\ \text{LC})\right|<0.5\\ \dfrac{1}{\left|\text{Mean}(1^{st}\ \text{LC})-\text{Mean}(2^{nd}\ \text{LC})\right|} & \text{if } \left|\text{Mean}(1^{st}\ \text{LC})-\text{Mean}(2^{nd}\ \text{LC})\right|>0.5\end{cases};$$

NV of eliminated feature sets

$$V_{NV10}=\left|\text{Mean}(5^{th}\ \text{LC})-\text{Mean}(6^{th}\ \text{LC})\right|;\ \text{("Mean" imply the mean value of the LC);}$$
$$V_{NV11}=\left|\text{Mean}(6^{th}\ \text{LC})-\text{Mean}(7^{th}\ \text{LC})\right|;$$
$$V_{NV12}=\left|\text{Mean}(7^{th}\ \text{LC})-\text{Mean}(8^{th}\ \text{LC})\right|;$$
$$V_{NV13}=\left|\text{Mean}(8^{th}\ \text{LC})-\text{Mean}(9^{th}\ \text{LC})\right|;$$
$$V_{NV14}=\left|\text{Var}(5^{th}\ \text{LC})\right|;$$
$$V_{NV15}=\left|\text{Var}(6^{th}\ \text{LC})\right|;$$
$$V_{NV16}=\left|\text{Var}(7^{th}\ \text{LC})\right|;$$
$$V_{NV17}=\left|\text{Var}(8^{th}\ \text{LC})\right|;$$
$$V_{NV18}=\left|\text{Var}(9^{th}\ \text{LC})\right|.$$

Note that if the TARMA (6, 3) model parameters are used directly as the feature set, it will be necessary to use a 6+3+1=10 (the additional one is related to the variance time evolution σ_t) time-varying component as the feature and no method can be used for feature reduction. In other words, in LC space it is possible and straightforward to choose the features that are most relevant for classification, but in other spaces,

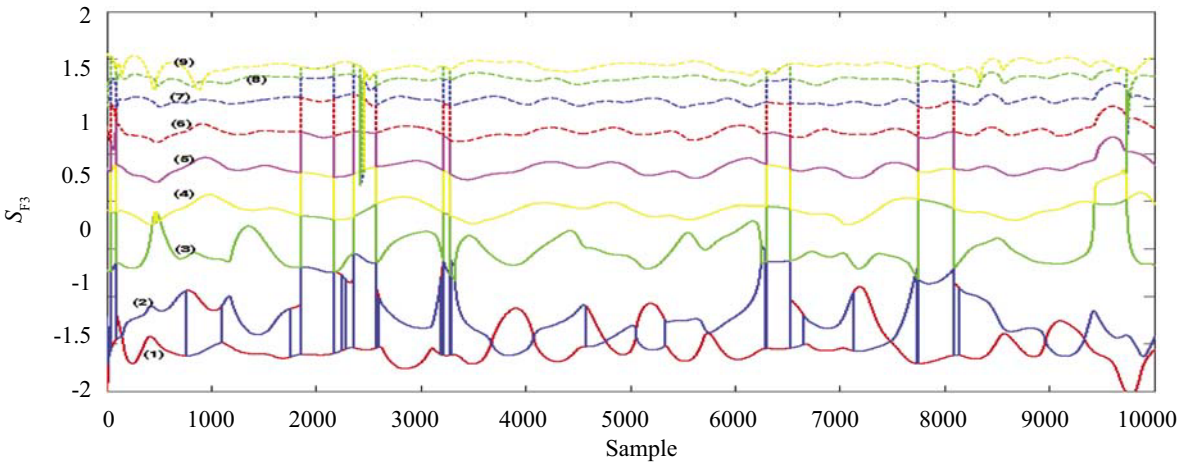

(a) Class 3

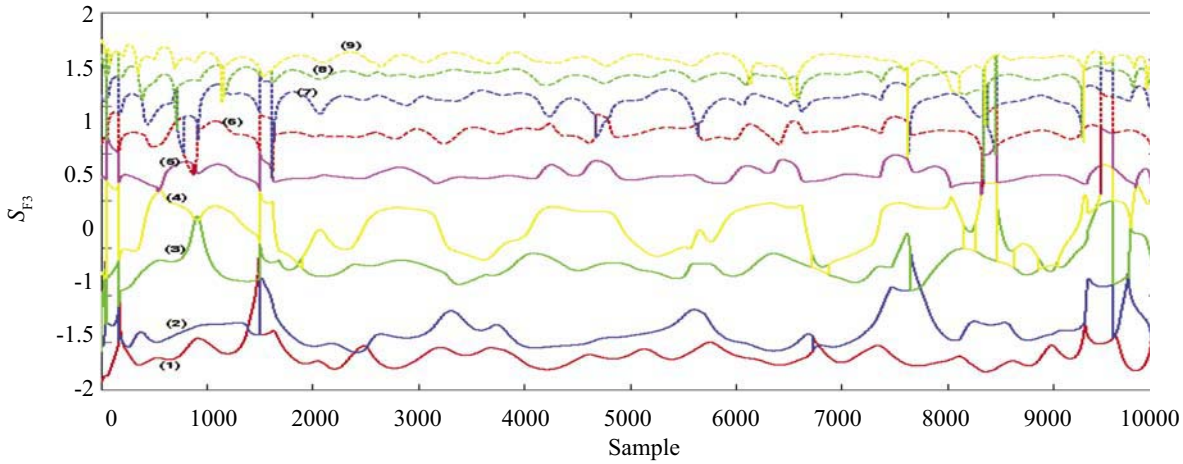

(b) Class 6

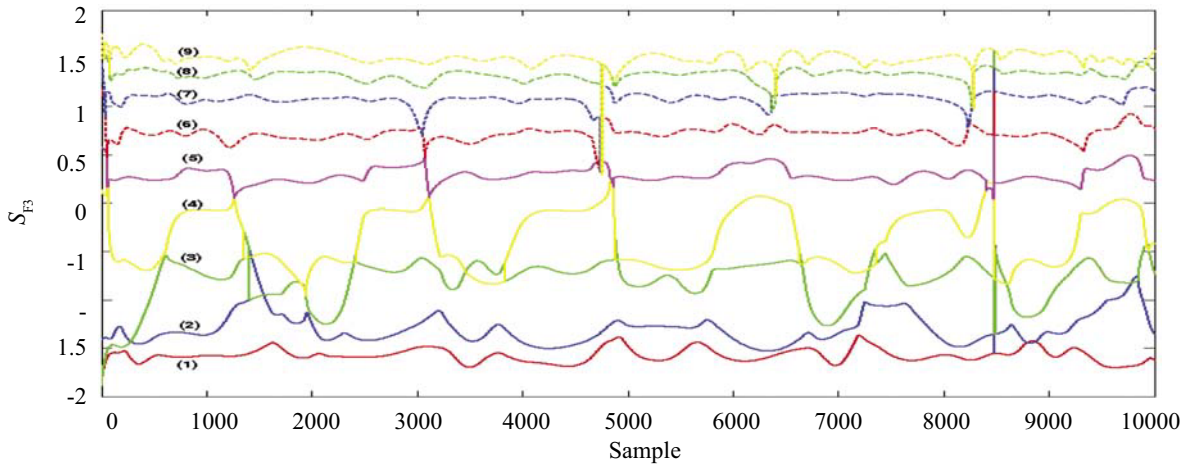

(c) Class 9

Fig. 3 Trajectories of extracted S_{F3}(FS3), associated with the obtained LCs, in order of decreasing IF from the bottom to top for different classes

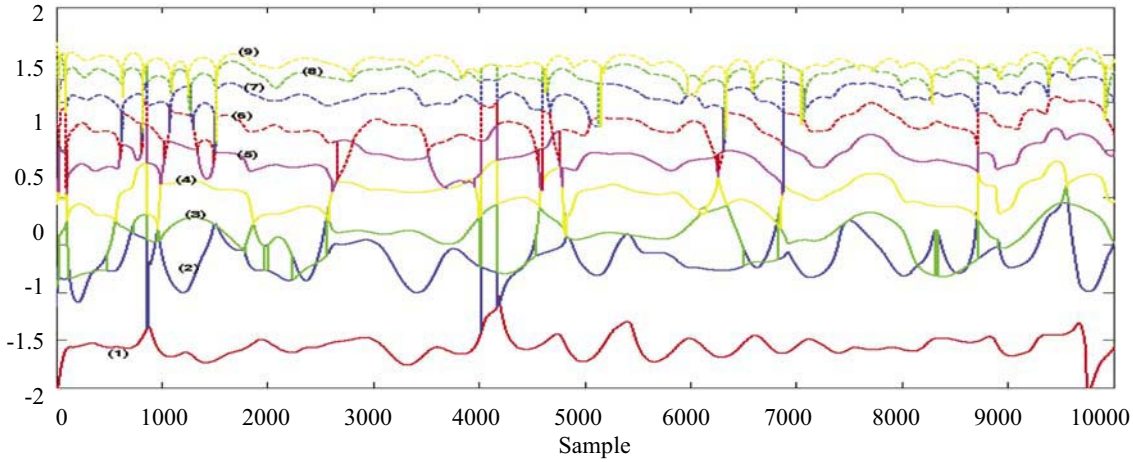

(d) Class 12

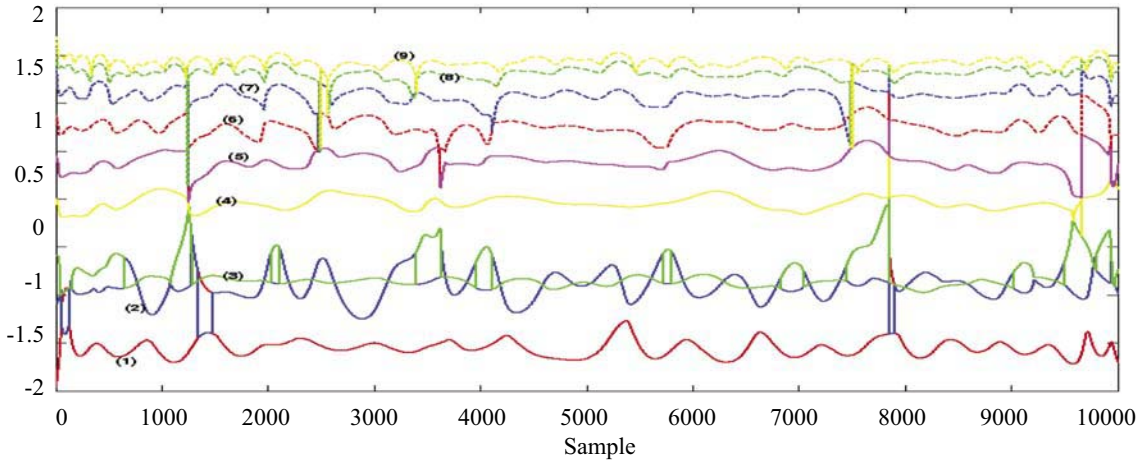

(e) Class 15

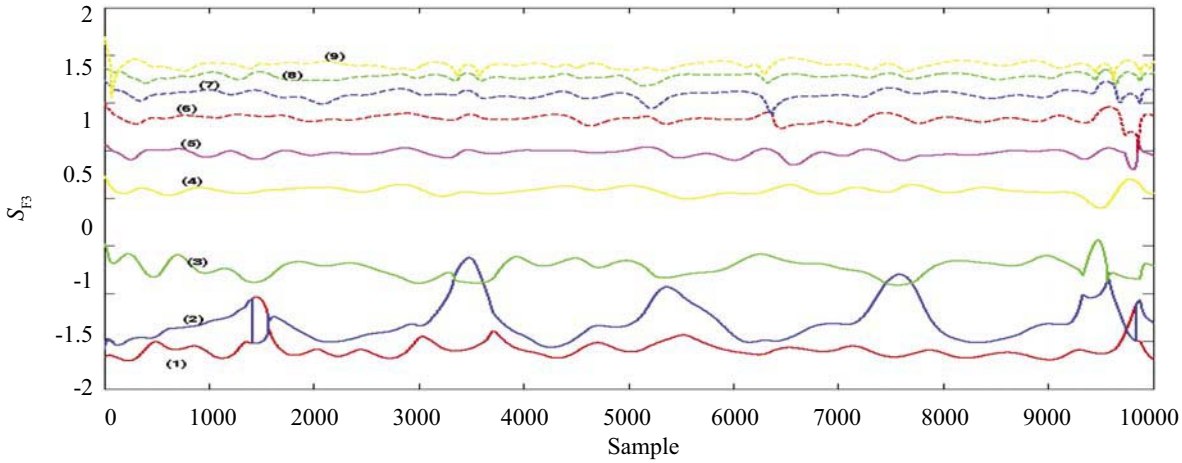

(f) Class 18

Fig. 3 (Continued)

accurate feature reduction is not achievable. In the next section, the extracted features are used as input to the FES for classification and the SR results are compared with the condition when different feature sets are employed.

3.3 Condition classification of the 3-DOF simulation system using FES

The extracted features from the LCs of the 3-DOF simulation system are considered as the inputs

to the global FES. The output of the global FES is the structure condition class number, defined in Table 1. The objective is to find a mapping between the inputs (features) and the output. The NV1 to NV8 are treated as fuzzy input variables. Fuzzy sets with Gaussian membership functions are used to define these input variables. The Gaussian membership function is defined as:

$$\mu(x)=\exp\left[-0.5\times\left[\frac{(x-m)}{\sigma}\right]^2\right] \tag{11}$$

where m is the mean-value and σ is the standard deviation. Gaussian fuzzy sets have the advantage of providing a smooth transition between the different sets. Furthermore, they always have nonzero values on the real number axes and therefore every rule in the FES applies to some degree. Rules for the FES are obtained by using the fuzzification method for the numerical values of the inputs. In this method, for each feature, corresponding to a given damage class, the degree of membership in the fuzzy set is calculated. Fuzzy rules represent a fuzzified model of the features obtained by an LC analysis for each damage class. Therefore, the fuzzy rules provide a knowledge base and represent how a human would interpret data to isolate a class using features. Once the fuzzy rules are applied for a given feature, there is a degree of membership for each class. For class isolation, the most likely class is the one with the highest degree of membership. The rules are set by employing the corresponding mean-values and standard deviations obtained by the method proposed in missing text. More details about using the FES as a classification tool are found in Pawar and Ganguli (2007) and/or Kosko (1997).

To evaluate the proposed method, NSV signals from the known classes of the 3-DOF system were produced, and based on each FS1, FS2 and FS3, the SR of classification was calculated. Also, numerical values of the all, retained and eliminated features were considered for each FS1, FS2 and FS3 to investigate the capability of the retained features in correct classification for different classes. The results are summarized in Table 2. As observed from this table, the SR of the test associated with FS3 is very high in comparison with FS1 or FS2. Moreover, regarding the SR, the retained features outperform the eliminated ones.

Table 2 SR of the classification when retained, eliminated and all of the features associated with FS1, FS2 and FS3 were used separately

Feature set	SR of the classification
S_{F1}	30% (retained features)
	20% (eliminated features)
	27% (all features)
S_{F2}	5% (retained features)
	1% (eliminated features)
	2% (all features)
S_{F3}	70% (retained features)
	34% (eliminated features)
	58% (all features)

4 Experimental setup and test

In this section, the proposed method is applied to a time-varying structure in the laboratory to assess the accuracy of the scheme in real systems.

4.1 Experimental set up for time-varying structure

As shown in Fig. 4, a simply supported beam with a varying mass on its mid-span is considered to be a time-varying system. To make the mass variable, sand is gradually poured into a container and mounted on the mid-span of the beam. The structure is excited by a shaker (B&K shaker type 4809) with band-limited white Gaussian noise as the ambient input, with a frequency range of 0 to 2.4 kHz. The acceleration signal (measured by B&K accelerometer type 4508) from a specific point of the beam is considered as the output. During the test, which lasted 20 seconds, one kg of sand flowed through the container. The signal acquisition was carried out by the B&K PULSE system (type 2827) with a sampling frequency set to 2048 Hz. The acceleration signal was low–pass filtered via a Chebyshev II filter with a cut-off frequency of 256 Hz, and re-sampled at 512 Hz. In order to minimize the initial and final effect of the response signal, the initial and final 1.5 seconds of the signal was discarded. Each structure condition class was considered by adding a spring or a mass with different values at different positions. The selected positions on the beam are denoted as points A and B in Fig. 5. The severity of each class was considered to be the corresponding value of the stiffness or mass. Referring to Table 3, 13 classes (including normal conditions) were considered to construct the fuzzy rules of FES in the training stage.

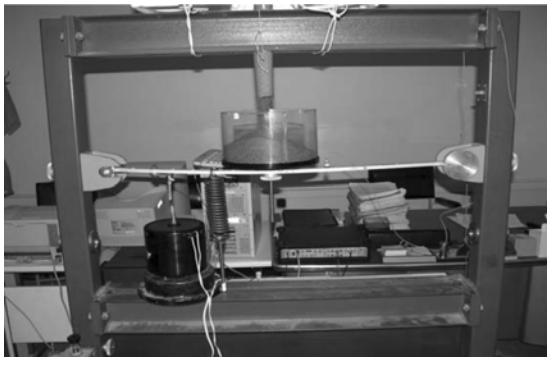

Fig. 4 Experimental set up

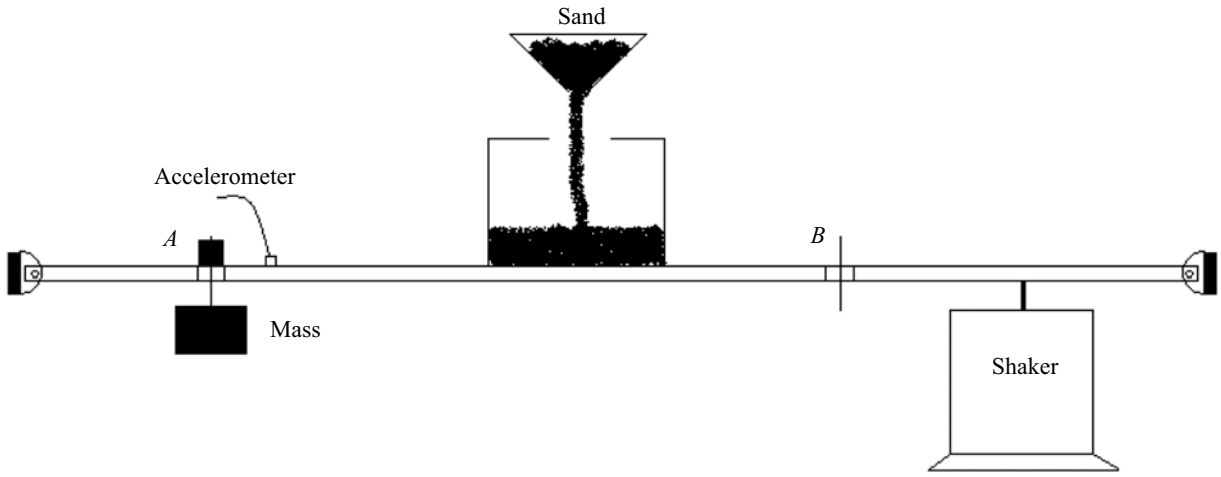

Fig. 5 Schematic view of the time-varying beam

Table 3 Linguistic classification of structure condition in the experimental system;

Class number	Rule	Stiffness/or mass value
1	Normal	–
2	Small mass in *A*	200g
3	Considerable mass in *A*	400g
4	High mass in *A*	600g
5	Small mass in *B*	200g
6	Considerable mass in *B*	400g
7	High mass in *B*	600g
8	Spring with small stiffness in *A*	3.7mm
9	Spring with considerable stiffness in *A*	4.2mm
10	Spring with high stiffness in *A*	5.0mm
11	Spring with small stiffness in *B*	3.7mm
12	Spring with considerable stiffness in *B*	4.2mm
13	Spring with high stiffness in *B*	5.0mm

Note: springs with the same materials, equal lengths and diameters, but with different wire diameters (3.7, 4.2 and 5 mm) are selected to simulate the damage severity

4.2 Feature extraction/reduction and condition classification

In this section, the NSV signal from the experiment was modeled by an FS-TARMA process. For this purpose, a proper structure of FS-TARMA model was selected by considering the number of natural frequencies in the working frequency range. By plotting the power spectrum of the simply supported beam without any time-varying mass in both the empty and full sand container (see Fig. 6), it was observed that in the frequency range of 0 to 256 Hz, there were three natural frequencies of the beam; therefore, the AR and MA part of the model was chosen as 6 (twice the number of natural frequencies) and 3, respectively. Also, after applying the method described in Section 2.2, the obtained AR, MA and innovations variance functional subspaces were found to be p_a=10, p_c=10 and p_s=10, respectively.

The LCs of the experimental NSV signal were derived by the proposed method similar to the method described in Section 3. In Fig. 7, trajectories of the extracted feature sets (FS1, FS2, and FS3) associated with the LCs obtained in order of decreasing IF, are illustrated for the normal class. Then, the LCs of the four highest modules, namely 4, 1, 3, and 2, were selected as the most informative ones (see Section 3.2). As an illustrative example, trajectories of FS3, associated with the LCs obtained for classes of 3, 6, 9, and 12 are shown in Figs. 8(a) to (d), respectively. Note that every class has its own characteristics. For example, for class 3, the third and fourth LCs are close to each other, as seen in Fig. 8(a). Also, in Fig. 8(b), there is interference between the second and third LC in class 6. Therefore, it

NV of all features
- NV of retained features
  - V_{NV1}=Mean(1st LC) ;
  - V_{NV2}=Mean(2nd LC);
  - V_{NV3}=Mean(3rd LC);
  - V_{NV4}=Mean(4th LC);
- NV of eliminated features
  - V_{NV5}=Mean(5th LC);
  - V_{NV6}=Mean(6th LC);
  - V_{NV7}=Mean(7th LC);
  - V_{NV8}=Mean(8th LC);
  - V_{NV9}=Mean(9th LC).

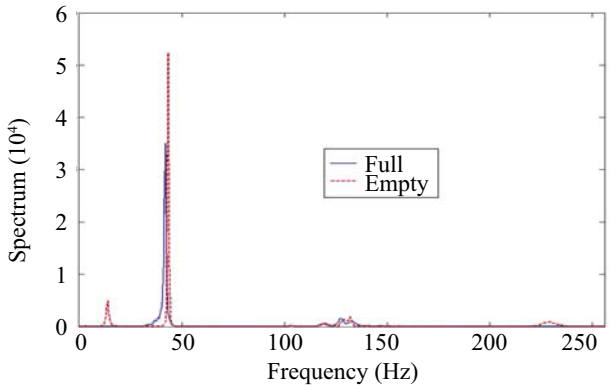

Fig. 6 FRF of the stationary beam (Normal) for empty and full container case

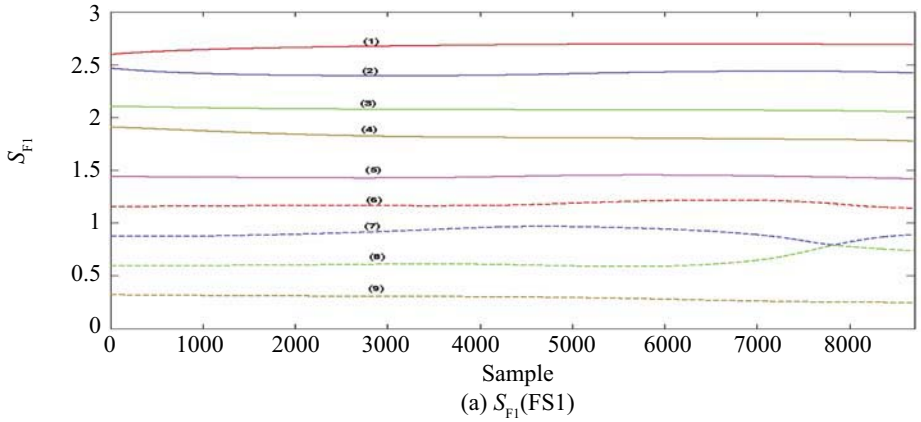

(a) S_{F1}(FS1)

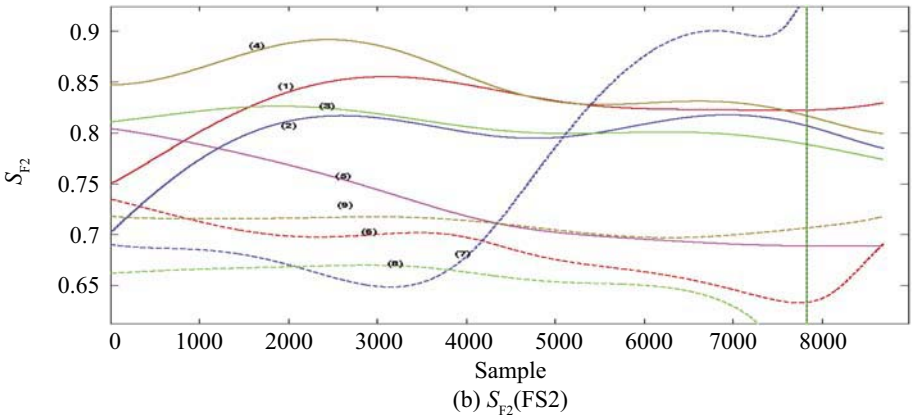

(b) S_{F2}(FS2)

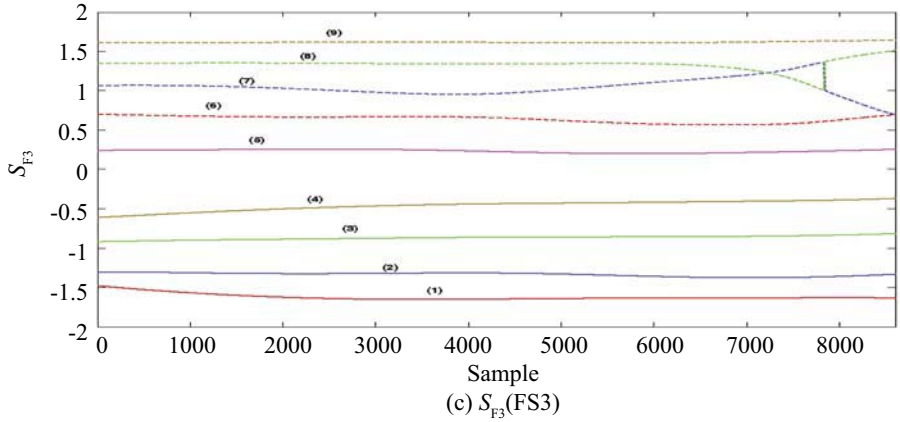

(c) S_{F3}(FS3)

Fig. 7 Trajectories of extracted feature sets, associated with the obtained LCs (The number of LCs is inside the parenthesis), in order of decreasing IF for different normal cases

is possible to classify the system condition according to the classes defined in Table 3, by defining the following numerical values of the extracted feature sets and using FES as described in Section 3.3:

To evaluate the efficiency of the proposed method used in the experimental study, signals from the known classes of the system were produced, and based on each FS1, FS2 and FS3, the SR of the classification was

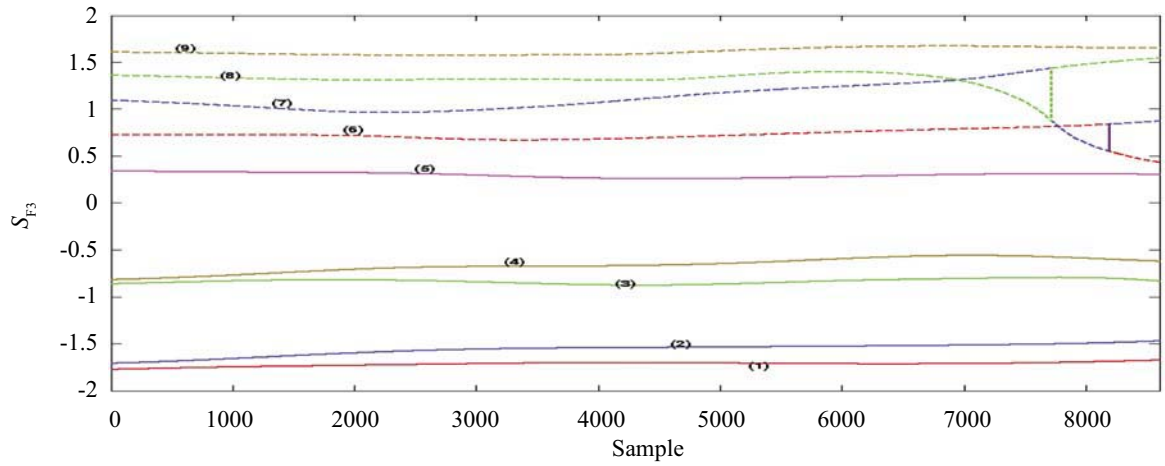

(a) Class 3

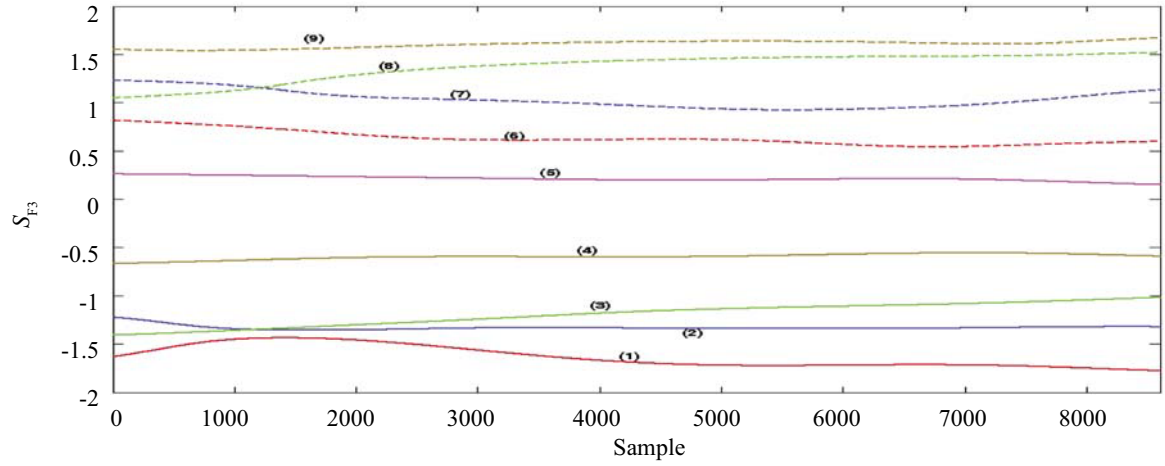

(b) Class 6

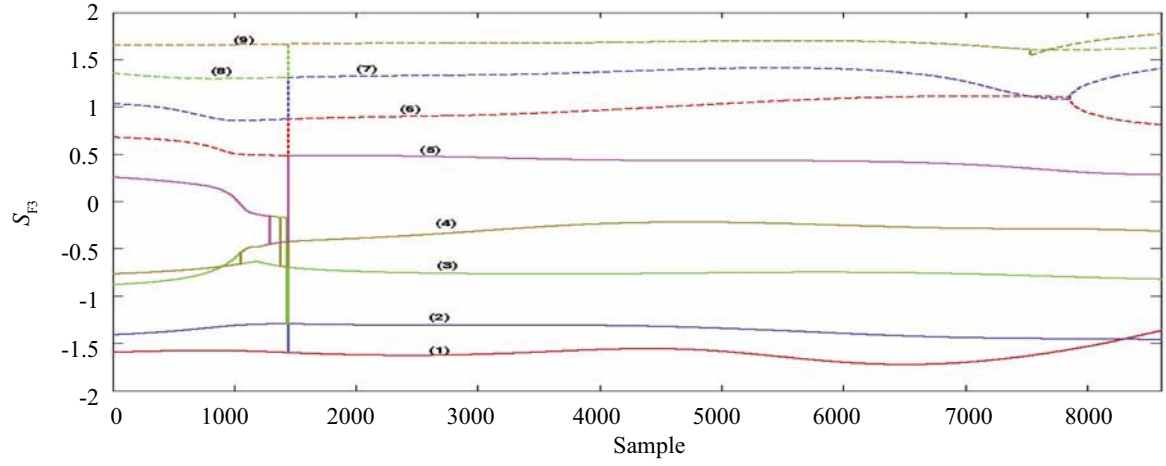

(c) Class 9

Fig. 8 Trajectories of extracted S_{F3}(FS3), associated with the obtained LCs, in order of decreasing IF from the bottom to top for different classes

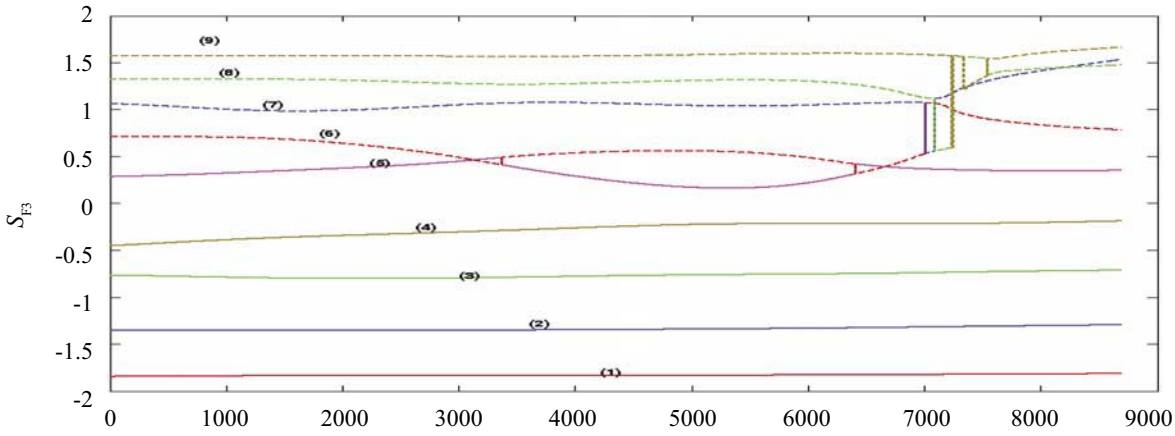

(d) Class 12

Fig. 8 (Continued)

calculated for all classes. The results are summarized in Table 4. As seen in this table, the SR of the test associated with the FS3 is very high compared with FS1 and FS2 and it also reduces the features increases the SR of the classification**.**

Table 4 SR of the classification when retained, eliminated and all of the features associated with FS1, FS2 and FS3 were used separately

Feature set	SR of the classification
FS1	32% (retained features) 16% (eliminated features) 21% (all features)
FS2	3% (retained features) 0.5% (eliminated features) 2% (all features)
FS3	60% (retained features) 21% (eliminated features) 46% (all features)

5 Conclusion

A new SHM method based on LC theory, and applied to decompose the structural NSV signal, feature extraction and reduction, is introduced. The first innovation of this work consists of the use of the advanced FS-TARMA model with DPE structure and 2SLS estimation method, known up to now as the most accurate method for structural modeling and analysis, for time-dependent parameters and innovation variance estimation. Then, the estimated parameters are used to decompose the signal of the time-varying structural system into components. The second innovation of this study is a novel feature extraction and reduction method for SHM based on a combination of the IM and IF, derived by decomposing the signal.

The proposed method is able to discriminate between the time-varying nature of the system parameters, and the damage that may occur in the course of operation which causes a change in the parameters. To evaluate the proposed method, a numerical simulation and laboratory testing of a time-varying structure were carried out, where different classes of damage were considered as the mass or stiffness of the structure varied from its nominal values. By applying FES as a suitable classification tool, it is shown that the SR of the proposed method provides correct classifications of different conditions of the structures.

References

Akaike H (1977), "On Entropy Maximization Principle," *Applications of Statistics*, **1**(1):27-41.

Draper NR and Smith H (1998), *Applied Regression Analysis*, 3rd ed., New York: John-Wiley.

Huang NE (1998), "The Empirical Mode Decomposition and the Hilbert Spectrum for Nonlinear and Non-stationary Time Series Analysis," *Proceedings of the Royal Society of London Series*, London, A 454, 903–995.

Kosko B (1997), *Fuzzy Engineering*, NJ: Prentice-Hall.

Li X and Du R (2005), "Condition Monitoring Using a Latent Process Model with an Application to Sheet Metal Stamping Processes," *Journal of Manufacturing Science and Engineering*, ASME, **127**:376-385.

Pawar PM and Ganguli R (2007), "Genetic Fuzzy System for Online Structural Health Monitoring of Composite Helicopter Rotor Blades," *Mechanical Systems and Signal Processing*, **21**: 2212-2236.

Poulimenos AG and Fassois SD (2003), "Estimation and Identification of Nonstationary Signals Using Functional Series TARMA Models," *Proceedings of the 13th IFAC Symposium on System Identification*, Rotterdam, The Netherlands, 162–167.

Poulimenos AG and Fassois SD (2005), "On the

Estimation of Nonstationary Functional Series TARMA Models," *Proceedings of the 13th European Signal Processing Conference*, Antalya, Turkey.

Poulimenos AG and Fassois SD (2006), "Parametric Time-domain Methods for Nonstationary Random Vibration Modelling and Analysis — A Critical Survey and Comparison," *Mechanical Systems and Signal Processing*, **20**: 763-816.

Prado R (1998), "Latent Structure in Nonstationary Time Series," *PhD thesi*s, Institute of Statistics and Decision Sciences, Duke University.

Qian S and Chen D (1996), *The Joint Time-frequency Analysis—Methods and Applications*, Englewood Cliffs, NJ: Prentice-Hall.

Rahimi N, Sadeghi MH and Mahjoob MJ (2007), "Performance of the Geometric Approach to Fault Detection and Isolation in SISO, SIMO and MIMO Systems," *Journal of Zhejiang University Science A*, **8**(9):1351-1526.

Sadeghi MH and Fassois SD (1997), Geometric Approach to the Nondestructive Identification of Fault in Stochastic Structural Systems, *AIAA Journal*, **35**(4): 700-705.

Sadeghi MH and Fassois SD (1998), "Reduced-dimensionality Geometric Approach to Fault Identification in Stochastic Structural Systems," *AIAA Journal*, **36**(12):2250-2256.

Sakellariou JS and Fassois SD (2006), "Stochastic Output Error Vibration-based Damage Detection and Assessment in Structures Under Earthquake Excitation," *Journal of Sound and Vibration*, **297**:1048-1067.

Serhat S and Emine A (2003), "Feature Extraction Related to Bearing Damage in Electric Motors by Wavelet Analysis," *Journal of the Franklin Institute*, **340**: 125-134.

Strang G and Nguyen T (1996), *Wavelets and filter banks*, Wellesley-Cambridge Press, USA.

Vincent HT, Hu S-LJ and Hou Z (1999), "Damage Detection Using Empirical Mode Decomposition Method and a Comparison with Wavelet Analysis," *Proceedings of the Second International Workshop on Structural Health Monitoring*, Stanford, 891-900.

West M and Harrison PJ (1997), *Bayesian Forecasting and Dynamic Models*, 2nd ed., New York: Springer-Verlag.

West M, Prado R and Krystal AD (1999) "Evaluation and Comparison of EEG Traces: Latent Structure in Nonstationary Time Series," *Journal of the American Statistical Association (Applications and Case Studies)*, **94**(446):375-387.

Yu Y, Dejie Y and Junsheng C (2006), "A Roller Bearing Fault Diagnosis Method Based on EMD Energy Entropy and ANN," *Journal of Sound and Vibration,* **294**: 269-277.

Zhan YM and Jardine AKS (2005), "Adaptive Autoregressive Mmodeling of Nonstationary Vibration Signals Under Distinct Gear States. Part 1: Modeling," *Journal of Sound and Vibration*, **286**: 429-450.

Zhan YM and Jardine AKS (2005), "Adaptive Autoregressive Modeling of Nonstationary Vibration Signals Under Distinct Gear States. Part 2: Experimental Analysis," *Journal of Sound and Vibration*, **286**:451-476.